SP-A Permeabilizes Lipopolysaccharide Membranes by Forming Protein Aggregates that Extract Lipids from the Membrane

Olga Cañadas,*† Ignacio García-Verdugo,* Kevin M. W. Keough,‡ and Cristina Casals*†
*Department of Biochemistry and Molecular Biology I, and †Centro de Investigaciones Biomédicas en Red Enfermedades Respiratorias, Complutense University of Madrid, Madrid, Spain; and ‡Department of Biochemistry and Discipline of Pediatrics, Memorial University of Newfoundland, St. John's, Newfoundland, Canada

ABSTRACT Surfactant protein A (SP-A) is known to cause bacterial permeabilization. The aim of this work was to gain insight into the mechanism by which SP-A induces permeabilization of rough lipopolysaccharide (Re-LPS) membranes. In the presence of calcium, large interconnected aggregates of fluorescently labeled TR-SP-A were observed on the surface of Re-LPS films by epifluorescence microscopy. Using Re-LPS monolayer relaxation experiments at constant surface pressure, we demonstrated that SP-A induced Re-LPS molecular loss by promoting the formation of three-dimensional lipid-protein aggregates in Re-LPS membranes. This resulted in decreased van der Waals interactions between Re-LPS acyl chains, as determined by differential scanning calorimetry, which rendered the membrane leaky. We also showed that the coexistence of gel and fluid lipid phases within the Re-LPS membrane conferred susceptibility to SP-A-mediated permeabilization. Taken together, our results seem to indicate that the calcium-dependent permeabilization of Re-LPS membranes by SP-A is related to the extraction of LPS molecules from the membrane due to the formation of calcium-mediated protein aggregates that contain LPS.

INTRODUCTION

The respiratory system is continually exposed to a wide array of toxic substances and infectious agents. Pulmonary surfactant is a lipid-protein complex that lines the air-liquid interface of alveoli, forming the first point of contact with inhaled microbial pathogens. Understanding the role of surfactant in host defense against respiratory infection is therefore of physiological importance. Surfactant protein A (SP-A), the most abundant protein by mass of pulmonary surfactant, has been shown to bind to a broad range of microorganisms, including Gram-negative and Gram-positive bacteria, fungi, viruses, and mite extract (1,2). The associations of lung collectins such as SP-A with pathogens result in bacterial aggregation, growth inhibition, and viral neutralization.

Recent studies have shown that SP-A directly inhibits the growth of Gram-negative bacteria such as *Escherichia coli*, *Bordetella pertussis*, and *Pseudomonas aeruginosa* by permeabilizing the bacterial membrane (3–6). In general, rough bacterial mutants containing truncated LPS species were more readily permeabilized by SP-A than smooth strains (3–5), and incorporation of rough, but not smooth, LPS into multilamellar liposomes composed of bacterial phospholipids (BPL) conferred susceptibility to SP-A-mediated permeabilization (7). It has been suggested that bacterial permeabilization and killing require interaction between SP-A and LPS, most likely through the protein binding to the proximal core and/or lipid A moieties of LPS (7). This hypothesis is supported by the finding that deletion of the terminal sugar of *B. pertussis* and *B. bronchiseptica* renders the organisms susceptible to aggregation and permeabilization by SP-A (4). On the other hand, several lines of evidence suggest that membrane rigidity plays an important role in the susceptibility of model bacterial membranes to SP-A. Incorporation of increasing amounts of cholesterol into *E. coli* Rc-LPS/1-palmitoyl-2-oleoyl-phosphatidylethanolamine liposomes produced a dose-dependent reduction in the level of permeabilization by human SP-A (7). In addition, comparative signature-tagged mutagenesis studies have recently shown that bacterial genes required to maintain membrane integrity play crucial roles in the resistance of *P. aeruginosa* to the permeabilizing effects of SP-A (5).

Using model bacterial membranes composed of *E. coli* Rc-LPS and 1-palmitoyl-2-oleoyl-phosphatidylethanolamine, Kuzmenko and co-workers (7) determined that SP-A permeabilizing activity is calcium-dependent and that the mechanism of permeabilization is different from that of melittin. These authors postulated that SP-A distorts or perturbs membrane structure, creating defects that allow small hydrophilic molecules to enter and traverse the bilayer. Despite considerable progress achieved in understanding the mechanism by which SP-A mediates permeabilization of LPS membranes, the molecular details of protein-induced membrane disruption remain poorly understood. This study was undertaken to obtain further information on the mechanisms of SP-A-mediated bacterial permeabilization. To that end, both monolayers and bilayers of Re-LPS were used as model membranes of Gram-negative bacteria.

Submitted May 13, 2008, and accepted for publication June 13, 2008.

Address reprint requests to Cristina Casals, PhD, Dept. of Biochemistry and Molecular Biology I, Faculty of Biology, Complutense University of Madrid, 28040 Madrid, Spain. Tel.: 34-91-3944261; Fax: 34-91-3944672; E-mail: ccasalsc@bio.ucm.es.

Editor: Paul H. Axelsen.

0006-3495/08/10/3287/08 $2.00

doi: 10.1529/biophysj.108.137323

MATERIALS AND METHODS

Materials

Rough LPS from *Salmonella minnesota* (serotype Re 595) was purchased from Sigma (St. Louis, MO, USA). The fluorescent labeling chemical sulforhodamine 101 sulfonyl chloride, Texas Red (TR), as well as the fluorescent lipid probe 1,6-diphenyl-1,3,5-hexatriene (DPH) were obtained from Molecular Probes Inc. (Eugene, OR, USA). The organic solvents (methanol and chloroform) used to dissolve rough LPS were HPLC-grade. All other chemicals were obtained from Sigma.

DPH concentration was determined spectrophotometrically by absorbance using a molar extinction coefficient in methanol of $\varepsilon^{350} = 88000\ M^{-1}cm^{-1}$. Re-LPS concentration was assessed by quantification of 2-keto-3-deoxy-octulosonic acid (KDO) (8). Water used in all experiments and analytical procedures was deionized and doubly distilled in glass, the second distillation being from dilute potassium permanganate solution.

Isolation and labeling of SP-A

SP-A was isolated from bronchoalveolar lavage of patients with alveolar proteinosis using a sequential butanol and octylglucoside extraction. The purity of SP-A was checked by one-dimensional SDS-PAGE in 12% acrylamide under reducing conditions and mass spectrometry (8). Quantification of SP-A was carried out by amino acid analysis in a Beckman System 6300 High Performance analyzer. The oligomerization state of SP-A was assessed by electrophoresis under nondenaturing conditions, electron microscopy, and analytical ultracentrifugation as reported elsewhere (9,10).

Fluorescently labeled SP-A was prepared as described by Ruano et al. (11). Briefly, SP-A in 5 mM Tris-HCl buffer, pH 8.3, was incubated with 1 mM TR (SP-A/TR molar ratio of 6:1) for 90 min in darkness at room temperature. To remove unreacted fluorescent reagent, the mixture was exhaustively dialyzed against 5 mM Tris-HCl, pH 7.4. Activity of labeled TR-SP-A compared to that of native protein was assayed by testing its ability to self-associate and to induce aggregation of DPPC and Re-LPS in the presence of calcium at 37°C as described elsewhere (8–10,12,13). The effect of TR-SP-A on π-A isotherms of Re-LPS monolayers was essentially identical (within our ability to measure) to that of nonconjugated SP-A.

Differential scanning calorimetry

For differential scanning calorimetry (DSC) measurements the lipid samples were prepared as aqueous dispersions. For this, rough LPS was suspended directly in 5 mM Tris-HCl, 150 mM NaCl, pH 7.4 (buffer A), containing either EDTA or $CaCl_2$, and allowed to swell for 1 h at a temperature above the gel-to-liquid phase transition temperature of the Re-LPS vesicles. Calorimetric measurements were performed as previously reported (14–16) in a Microcal VP differential scanning calorimeter (Microcal Inc., Northampton, MA, USA) at a heating rate of 0.5°C/min. Re-LPS aqueous dispersions (0.4 mM), in the absence and presence of different amounts of SP-A, were loaded in the sample cell of the microcalorimeter with 0.6 mL of buffer A in the reference cell. Four calorimetric scans were collected from each sample between 10°C and 50°C. The standard Microcal Origin software was used for data acquisition and analysis. The excess heat capacity functions were obtained after subtraction of the buffer-buffer baseline.

DPH fluorescence measurements

Steady-state fluorescence measurements were carried out using an SLM-Aminco AB-2 spectrofluorimeter equipped with a thermostatted cuvette holder ($\pm$ 0.1°C) (Thermo Spectronic, Waltham, MA, USA), with 5 $\times$ 5 mm path-length quartz cuvettes, as previously described (14). The required amount of DPH dissolved in methanol was added to Re-LPS dissolved in chloroform/methanol/water 17:7:1 (v/v) (probe/Re-LPS molar ratio of 1:200, final Re-LPS concentration of 1 mg/mL). The solvent was removed under a stream of nitrogen before addition of buffer A, which contained either 150 μM EDTA or 150 μM $CaCl_2$. The sample was allowed to hydrate for 1 h at a temperature above the gel-to-liquid phase transition temperature of Re-LPS suspension (45°C). To reduce the size of Re-LPS particles, the sample was sonicated at 45°C for 4 min at 390 W/cm^2 (bursts of 0.6 s, 0.4 s between bursts) in a UP 200S sonifier, with a 2-mm microtip. Exposure to light was minimized throughout the preparation of Re-LPS aqueous dispersions doped with DPH. An appropriate amount of SP-A in buffer was added to each aliquot of Re-LPS dispersions to give the desired final concentration of protein, with less than a 5% increase in volume for each aliquot. For DPH fluorescence intensity measurements, the emission spectra were recorded with the emission polarizer set at the magic angle ($m = 54.7°$) relative to the vertically polarized excitation beam. This was done to reduce contributions from scattering due to Re-LPS dispersions and to avoid intensity artifacts due to molecular rotation during the lifetime of the excited state (17). Moreover, background intensities in probe-free samples were subtracted from each recording of fluorescence intensity. Measurements were performed at 15°C, 25°C, and 37°C.

Epifluorescence microscopy

Epifluorescence microscopy measurements were performed on a surface balance whose construction and operation have been described previously (18). Monolayers were prepared by spreading Re-LPS onto a buffer A subphase containing either 150 μM $CaCl_2$ or 150 μM EDTA, with or without 0.08 μg/mL of TR-SP-A, as reported elsewhere (19). The use of low Ca^{2+} concentrations prevents extensive protein self-aggregation that occurs at higher Ca^{2+} concentrations (13). Extensive SP-A self-aggregation hampers the interaction of SP-A with lipid films (20).

After a 1-h period, which allowed for solvent evaporation and penetration of the protein into the gas or gas-liquid expanded coexistence phases, the monolayer was compressed. At selected surface pressures, a video recording of TR fluorescence was made for a 1-min period. The video images were obtained with a CCD camera, which records in black and white. Images were analyzed with digital image processing using JAVA 1.3 software (Jandel Scientific, San Rafael, CA) as discussed elsewhere (11,18).

Pressure-area isotherms and relaxation kinetics of Re-LPS monolayers

Surface pressure-area isotherms of Re-LPS films were measured using a thermostated Langmuir-Blodgett trough (102M micro Film Balance, NIMA Technologies, Coventry, United Kingdom) equipped with an injection port and magnetically stirred. The trough, of a total area of 100 cm^2, is equipped with two symmetrical movable barriers controlled by an electronic device, which allows barrier movement at constant speed. Re-LPS dissolved in chloroform/methanol/water 17:7:1 (v/v) was spread onto a buffer A subphase containing either 150 μM $CaCl_2$ or 150 μM EDTA. The lipid monolayers were allowed to equilibrate for 15 min before the injection of SP-A into the subphase to yield a final protein concentration of 0.1 μg/mL (SP-A/Re-LPS weight ratio of 1%). After a 1-h period, which allowed for solvent evaporation and penetration of the protein into the gas or gas-liquid expanded coexistence phases, the monolayer was compressed. A barrier speed of 50 cm^2/min has been chosen as the optimum velocity for the film compression. Our preliminary experiments showed rather poor reproducibility of Re-LPS monolayers when a lower compression speed (10 and 35 cm^2/min) was used, whereas a higher velocity (60 cm^2/min) profoundly affected the collapse characteristics. The surface areas in the trough before and after compression were 76 and 22 cm^2, respectively. The data shown represent the average of seven measurements. All measurements were performed at 25°C.

To determine SP-A's effects on the relaxation kinetics of Re-LPS monolayers, the Re-LPS organic solution was spread onto a buffered saline subphase by microsyringe. After 15 min the monolayer was compressed to a preset surface pressure kept constant by automatically adjusting the surface area of the trough through the movement of barriers. Once the desired surface

pressure was reached, SP-A was injected into the subphase. A relaxation curve was obtained by recording the trough surface area during the relaxation period.

RESULTS

SP-A decreases van der Waals interactions between Re-LPS acyl chains

To gain insight into the mechanism of SP-A-promoted bacterial membrane permeabilization, we explored SP-A's effects on the physical properties of rough lipopolysaccharide membranes using DSC. To obtain further information on the role that calcium ions play in Re-LPS/SP-A interaction, aqueous dispersions of Re-LPS were prepared in buffer A containing either EDTA or calcium. In the presence of 150 μM EDTA, the Re-LPS thermogram was characterized by a phase transition with a gel-to-liquid phase transition characterized by a melting temperature (T_m) of 24.5°C and a transition enthalpy of 4.2 kcal/mol (Fig. 1 and Table 1). When 1 wt % SP-A was added to Re-LPS membranes, no SP-A-induced effects on the T_m were observed, but the overall transition enthalpy of Re-LPS membranes decreased by ~21% (Fig. 1 and Table 1). Remarkably, greater amounts of SP-A (2.5 wt %) had no effect on either the T_m, the onset temperature, or the transition enthalpy with respect to Re-LPS alone. This might be because of electrostatic repulsions between negative charges in the SP-A surface and the negatively charged Re-LPS molecules at such protein concentrations, which would prevent the interaction of the protein with Re-LPS. In this regard, we have previously shown that at low SP-A concentrations the protein interacts with the negatively charged DPPC/1-palmitoyl-2-oleoyl-phosphatidylglycerol/palmitic acid vesicles (16). However, as the amount of SP-A increases, the interaction of the protein with these membranes is hindered by electrostatic repulsions between SP-A and negatively charged lipids (16).

On the other hand, in the presence of 150 μM $CaCl_2$, the Re-LPS thermogram was characterized by a complex double peak, indicative of calcium-induced lipid phase separation (Fig. 1 and Table 1). When SP-A was added, the overall transition enthalpy sharply decreased (~67% at SP-A/Re-LPS weight ratio of 1% and ~78% at 2.5 wt % SP-A) (Fig. 1 and Table 1). In the presence of 2.5 wt % SP-A there was a very small increase in the transition onset temperature, which was also reflected in the T_m. At saturating calcium concentrations (5 mM), the calorimetric endotherm of Re-LPS was characterized by a single gel-to-liquid crystalline phase transition, which became narrower and shifted to higher temperatures (T_m = 36.4 ± 0.2°C) (data not shown). This indicates stabilization of the gel phase. Under these conditions, extensive self-aggregation of SP-A induced by calcium might prevent their interaction with the membrane, since 1 wt % SP-A decreased the transition enthalpy by only 24% (data not shown). On the other hand, the greater effect of SP-A at low (150 μM) rather than high (5 mM) calcium concentrations might also be because of the presence of lipid phase separation within the Re-LPS membrane at 150 μM Ca^{2+}. The coexistence of gel/fluid lipid phases might confer susceptibility to SP-A-mediated membrane disruption since SP-A can insert into or perturb the membrane at the dislocations of the domain boundaries.

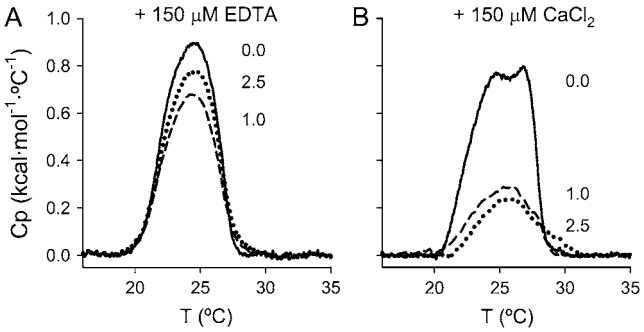

FIGURE 1 Effect of SP-A on the DSC heating scans of Re-LPS membranes (0.4 mM) in buffer A containing either 150 μM EDTA (*A*) or 150 μM $CaCl_2$ (*B*). Experiments were performed in the presence of different SP-A/Re-LPS weight ratios: 0% (*solid line*), 1% (*dashed line*), and 2.5% (*dotted line*). Calorimetric scans were performed at a rate of 0.5°C/min. Data shown are the means of four thermograms.

TABLE 1 Effect of SP-A on the phase transition parameters determined for Re-LPS vesicles (0.4 mM) in buffer A containing either 150 μM EDTA or 150 μM $CaCl_2$

Sample	SP-A wt %	T_m ± SD (°C)	ΔH ± SD (kcal/mol)
Re-LPS (150 μM EDTA)	0.0	24.5 ± 0.2	4.2 ± 0.3
	1.0	24.4 ± 0.2	3.3 ± 0.3
	2.5	24.6 ± 0.2	3.8 ± 0.3
Re-LPS (150 μM $CaCl_2$)	0.0	24.4/26.9 ± 0.2	3.3/1.2 ± 0.3
	1.0	25.7 ± 0.2	1.5 ± 0.3
	2.5	25.6 ± 0.2	1.0 ± 0.3

Data are taken from heating scans. Values are the means ± SD of three experiments.

Together, these results show that SP-A decreases the transition enthalpy of Re-LPS membranes in both the absence and presence of calcium. This might be explained by a reduction in van der Waals interactions between LPS acyl chains. The SP-A effect on the transition enthalpy of Re-LPS membranes seemed to be stronger in membranes with lipid phase separation induced by calcium.

SP-A favors the penetration of water molecules in Re-LPS membranes

To determine whether the SP-A-induced reduction of LPS-LPS interactions described above is related to the permeabilization of Re-LPS membranes, we explored SP-A/Re-LPS interactions using the fluorescent dye DPH. DPH fluorescence is very sensitive to the polarity of the membrane environment. This probe has a low quantum yield and a very short lifetime when exposed to water. Thus, its fluorescence is

sensitive to the amount of water that penetrates into the lipid bilayer. Since SP-A's effects on the thermotropic properties of Re-LPS membranes were studied in the absence and presence of calcium ions, we first examined calcium effects on the fluorescence intensity of DPH embedded in Re-LPS aqueous dispersions. Fig. 2 *A* shows that in the presence of 150 μM calcium (discontinuous line), the fluorescence intensity of DPH in Re-LPS suspensions was lower than in its absence (continuous line). This effect might be due to the calcium-induced lipid phase separation described above, which would favor the accessibility of water molecules to the probe. As a result, DPH fluorescence is quenched. In fact, at saturating calcium concentrations, the fluorescence of DPH increased with respect to that obtained in the presence of 150 μM $CaCl_2$ because of the more tight packing of the Re-LPS acyl chains plus the lack of domain separation with attendant boundary dislocations (data not shown).

Fig. 2 *B* shows the fluorescence intensity of DPH embedded in Re-LPS membranes as a function of SP-A concentration at 25°C, in both the absence and presence of calcium. The addition of very small amounts of SP-A (0.5 wt %) to aqueous suspensions of Re-LPS lacking calcium decreased the fluorescence of the dye (Fig. 2 *B*, *open triangles*). However, with increasing SP-A concentrations, a dose-dependent recovering of DPH fluorescence was observed. The absence of SP-A effect on DPH fluorescence at high protein concentrations (2.5 wt %) might be because of increased electrostatic repulsions between SP-A and Re-LPS molecules as described above. On the other hand, the addition of increasing amounts of SP-A to Re-LPS vesicles in the presence of 150 μM $CaCl_2$ led to a dose-dependent decrease in the fluorescence intensity of DPH (~70% at SP-A/Re-LPS weight ratio of 2.5%) (Fig. 2 *B*, *solid circles*). This decrease in DPH fluorescence intensity may be due to water penetration in the Re-LPS bilayer as a consequence of SP-A-induced Re-LPS membrane destabilization. At saturating calcium concentrations, the addition of increasing amounts of SP-A led to a decrease of the fluorescence signal by only ~30% (data not shown). To test whether the coexistence of solid and fluid phases in LPS membranes confers susceptibility to SP-A-mediated quenching of DPH fluorescence, we measured the effect of SP-A on DPH fluorescence in the presence of 150 μM $CaCl_2$ at different temperatures. We found that DPH fluorescence was less affected by SP-A at temperatures below (15°C) and above (37°C) the T_m of Re-LPS vesicles rather than close to it (25°C) (data not shown). Thus, it is reasonable to conclude that SP-A-mediated water penetration in Re-LPS model membranes was favored by the coexistence of gel and fluid lipid phases in these membranes. This is consistent with the finding that the presence of lipid phase separation within the Re-LPS membrane conferred susceptibility to SP-A-mediated membrane disruption as described above.

SP-A forms interconnected aggregates on the surface of Re-LPS monolayers in the presence of calcium

To gain insight into SP-A/LPS interaction, we performed epifluorescence measurements with a fluorescent derivative of SP-A (TR-SP-A). In the absence of calcium, TR-SP-A fluorescence appeared below the monolayers at low surface pressures (4.5 mN/m) (Fig. 3). Above this pressure the fluorescence of TR-SP-A was randomly distributed in the film, forming fluorescent structures with amorphous morphology adsorbed at the polar surface of LPS monolayers (Fig. 3). The interactions between the lipids and the protein led to the formation of an unstable lipoprotein film that can be observed in compression isotherms (Fig. 4 *A*).

On the other hand, in the presence of 150 μM calcium, TR-SP-A fluorescence appeared in the film at lower surface pressures (2.8 mN/m) than in its absence (Fig. 3), which indicates that this cation modified the interaction of SP-A with Re-LPS and allowed the association of SP-A with the monolayer at lower surface pressures. At 3.9 mN/m, bright fluorescent regions of TR-SP-A aggregates appeared in Re-LPS monolayers. As the pressure increased, the intense rings of TR fluorescence became interconnected. These results show that SP-A has different modes of interaction with Re-LPS monolayers in the absence and presence of calcium. Calcium promoted the self-aggregation of the protein (13),

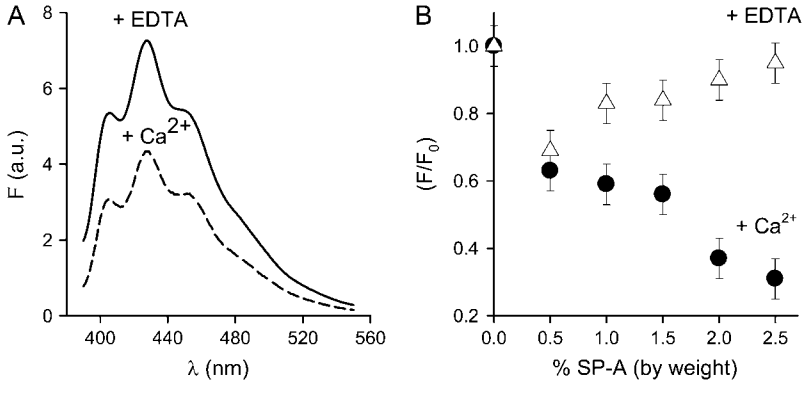

FIGURE 2 (*A*) DPH fluorescence intensity of Re-LPS membranes (0.4 mM) in buffer A containing either 150 μM EDTA or 150 μM $CaCl_2$. At this Ca^{2+} concentration, there is calcium-induced lipid phase separation at 25°C, as shown in Fig. 1. The fluorescent probe DPH partitions evenly into fluid and solid domains, and its fluorescence is sensitive to the amount of water that penetrates into Re-LPS membranes. (*B*) DPH fluorescence as a function of SP-A concentration. F and F_0 are the corrected emission intensities at 430 nm (λ_x= 340 nm) in the presence and absence of SP-A, respectively. Experiments were performed in the presence of 150 μM EDTA (Δ) or 150 μM $CaCl_2$ (●), at 25°C. The DPH/Re-LPS molar ratio was 1:200 in all samples. The Re-LPS concentration was 1 mg/mL (0.4 mM). All data points are the mean values of experiments performed in triplicate (± SD).

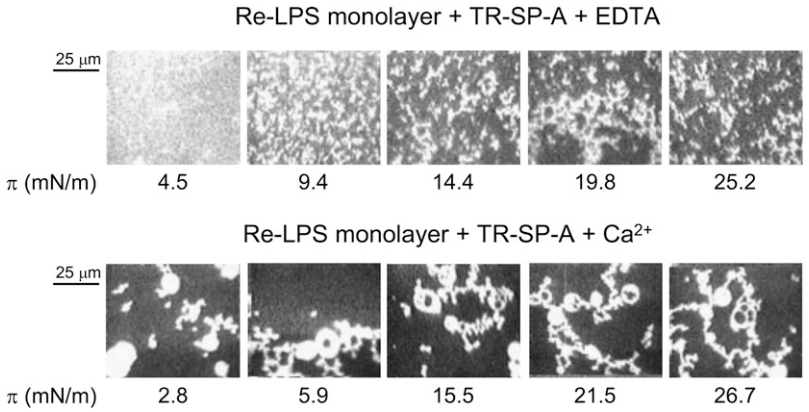

FIGURE 3 Typical epifluorescence microscopic images obtained from Re-LPS monolayers spread on a buffer A subphase containing fluorescent TR-SP-A and either 150 μM EDTA or 150 μM $CaCl_2$. The images were recorded through a filter that selects fluorescence coming from Texas Red (emission centered at 590 nm) at different surface pressures. The bright regions indicate the phase containing the fluorescently labeled SP-A. The scale bar is 25 μm.

which allowed the achievement of high local protein concentrations.

SP-A destabilizes Re-LPS monolayers

Fig. 4 shows the surface pressure-area (π-A) isotherms obtained at 25°C for monolayers of Re-LPS in the absence (*A*) and presence (*B*) of calcium, and with and without SP-A. In the absence of calcium (Fig. 4 *A*), the compression isotherms of Re-LPS monolayers revealed smooth π-A curves lacking indications for structural transitions (Fig. 4 *A*, *solid line*). This might suggest that the films are in the liquid expanded (LE) state. However, coexisting LE and liquid condensed (LC) domains in Re-LPS monolayers have been observed by atomic force microscopy (21). At a surface pressure of 56 mN/m, Re-LPS films collapsed. When 0.1 μg/mL SP-A (1 wt %) was present in the subphase, an expansion of the isotherm was observed (Fig. 4 *A*, *solid circles*), which indicates perturbation of lipid packing by the protein. The collapse of the Re-LPS/SP-A film took place at surface pressures lower than that of pure Re-LPS. This suggests that SP-A likely promoted membrane destabilization.

In the presence of 150 μM calcium (Fig. 4 *B*), the compression isotherm of Re-LPS was shifted to lower molecular areas with respect to that obtained in the absence of the divalent cation (Fig. 4 *A*). The compression isotherm of Re-LPS films showed a kink at 36 mN/m (Fig. 4 *B*, continuous line), which suggests the appearance of a phase transition (LE-LC). Calcium might facilitate the transition from a disordered phase (LE) to a more ordered phase (LC). This might be attributed to the electrostatic interactions between the negatively charged groups of Re-LPS and calcium ions, as well as to dehydration effects induced by the presence of $CaCl_2$. Attempts to visualize this transition by epifluorescence microscopy of Re-LPS monolayers containing NBD-PC did not succeed, since epifluorescence images show that the fluorescence of NBD-PC was uniform over the monolayer surface (data not shown). This would signify that solid domains have much smaller dimensions than the optical resolution. With respect to the collapse pressure of Re-LPS films, we found that it was higher in the presence of calcium (60 mN/m) than in its absence (56 mN/m). This indicates that calcium induces stabilization of the monolayer or that EDTA destabilizes the monolayer due to the EDTA-induced weakening of LPS-LPS interactions (22).

On the other hand, the presence of 0.1 μg/mL SP-A in the subphase expanded the isotherm (Fig. 4*B*, *solid circles*) to a lesser extent than in the presence of EDTA (Fig. 4 *A*, *solid circles*). This might be because of the calcium-induced charge neutralization, which would minimize the electrostatic repulsions between SP-A and Re-LPS. In addition, SP-A decreased the collapse pressure of Re-LPS monolayers (Fig. 4 *B*, *solid circles*), which indicates that SP-A destabilized the interfacial film in the presence of calcium.

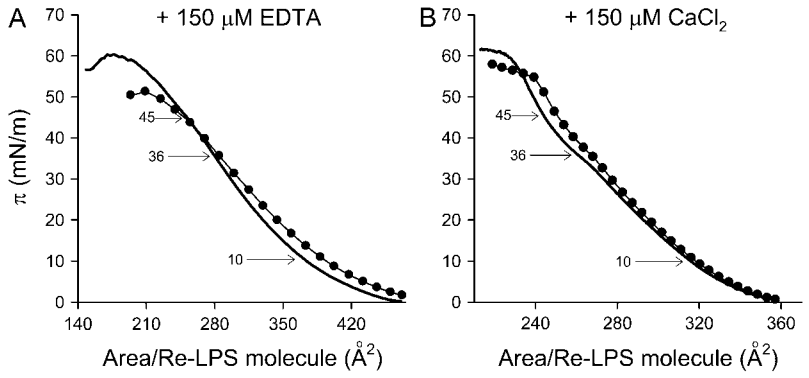

FIGURE 4 Effect of SP-A on the pressure-area isotherms of Re-LPS monolayers spread onto a buffered saline subphase containing either 150 μM EDTA (*A*) or 150 μM $CaCl_2$ (*B*). The % SP-A/Re-LPS weight ratio is 0 (solid line) and 1 (solid circles), which corresponds to SP-A concentrations of 0 and 0.1 μg/mL, respectively. The temperature of the subphase was 25.0°C $\pm$ 0.1°C. Data shown are the means of seven independent measurements. The SD for each isotherm was too small to be displayed by error bars.

SP-A induces Re-LPS molecular loss

To characterize the mechanism of Re-LPS membrane destabilization by SP-A, the relaxation time of the surface area of Re-LPS films was measured after compression to different surface pressures, in both the absence and presence of 0.1 μg/mL SP-A. From the DSC and DPH fluorescence measurements described above (Figs. 1 and 2, respectively) we infer that the SP-A-induced destabilization of LPS membranes in the presence of Ca^{2+} is facilitated by the presence of gel/fluid phase coexistence in the membrane. Thus, Re-LPS monolayers at 25°C were compressed to 10 mN/m (LE phase), 36 mN/m (LE/LC phase coexistence), and 45 mN/m (LC phase). Fig. 5 shows the typical relaxation curves for Re-LPS films at these surface pressures in the presence of 150 μM $CaCl_2$, with (solid circles) and without (open circles) 0.1 μg/mL SP-A. Pure Re-LPS monolayers exhibited an unstable behavior, with considerable area loss during the relaxation period at all surface pressures studied (Fig. 5, *open symbols*). Thus, within 20 min, the area loss at both 10 and 45 mN/m was ~25%, whereas at 36 mN/m the rate of area loss increased substantially and films at 36 mN/m were the least stable, with area loss of ~53% within 20 min.

The presence of 0.1 μg/mL SP-A in the subphase increased the relaxation rate of Re-LPS monolayers at all surface pressures studied (Fig. 5, *solid symbols*). As a result the area loss at a given time was greater in the presence than the absence of SP-A. This effect was stronger at 36 mN/m, at which LE and LC phases coexist, with an area loss of 40% within 6 min. This supports the finding that the SP-A-induced destabilization of Re-LPS membranes is favored by the coexistence of gel and fluid lipid phases within the LPS membrane. On the other hand, in the presence of 150 μM EDTA, monolayer instability markedly increased (data not shown). The addition of 0.1 μg/mL SP-A in the presence of 150 μM EDTA did not affect the relaxation kinetics of Re-LPS films compressed to 10 mN/m (data not shown). Re-LPS monolayers compressed to higher surface pressures became so unstable that it was not possible to determine SP-A's effects on the relaxation kinetics of Re-LPS monolayers. The fact that SP-A affected the relaxation kinetics of Re-LPS films, compressed to 10 mN/m, in the presence of calcium, but not in its absence, seems to indicate that the SP-A-induced destabilization of Re-LPS membranes is calcium-dependent.

Two possible processes might account for the area loss of Re-LPS monolayers described above: the transformation of the two-dimensional (2D) monolayer material into three-dimensional (3D) aggregates (23,24), and the dissolution of lipid molecules into the subphase through diffusion (25). According to a model proposed by Smith and Berg (25), if the monolayer molecular loss is because of dissolution of Re-LPS molecules into the subphase, a linear relationship between $-\log(A/A_0)$ and the square root of time, $\sqrt{t}$ would be obtained, where A and A_0 are the trough surface areas at a given time, t, and at $t = 0$, respectively. Thus, to discriminate between desorption and the nucleation and growth of 3D aggregates, the variance of $-\log(A/A_0)$ with $\sqrt{t}$ was plotted for Re-LPS films in the absence and presence of SP-A (Fig. 6). The absence of a linear relationship of Re-LPS data, with and without SP-A, indicates that at all surface pressures studied, the area loss during the relaxation was caused by the formation of 3D aggregates but not by the dissolution of Re-LPS molecules into the subphase. These results are in agreement with previous findings of Garidel and co-workers (26), who showed that unilamellar/cubic inverted aggregate structures of Re-LPS are converted into multilamellar structures by divalent cations. Since in the presence of calcium large protein aggregates were observed on the surface of Re-LPS monolayers (Fig. 3), it is conceivable that the calcium-dependent permeabilization of Re-LPS membranes by SP-A is related to the formation of calcium-mediated lipid-protein aggregates that extract LPS molecules from the membrane. This would mean fewer LPS molecules per unit of area, which would cause the membrane to be less tightly packed and permeable.

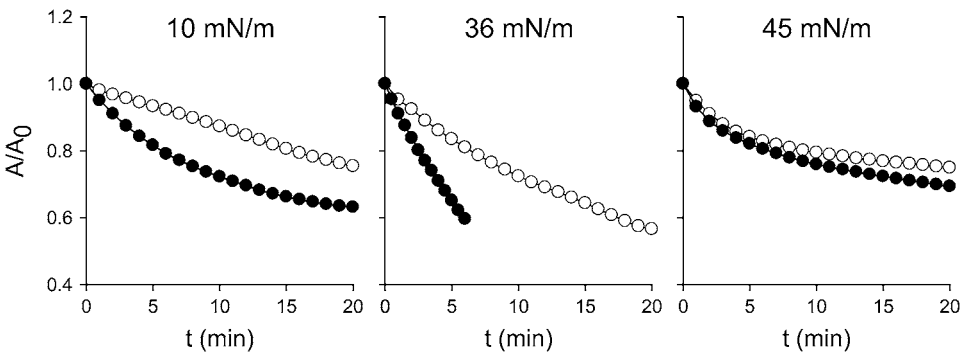

FIGURE 5 Effect of SP-A (0.1 μg/mL) (*solid circles*) on the relaxation kinetics of Re-LPS monolayers (*open circles*) spread onto a saline subphase containing 150 μM $CaCl_2$ and compressed to different surface pressures: 10 mN/m (LE phase), 36 mN/m (LE/LC phase coexistence), and 45 mN/m (LC phase). A and A_0 are the trough surface areas at a given time, t, and at $t = 0$, respectively. The temperature of the subphase was 25.0°C ± 0.1°C. Data shown are the means of seven independent measurements. The SD for each relaxation kinetic was too small to be displayed by error bars.

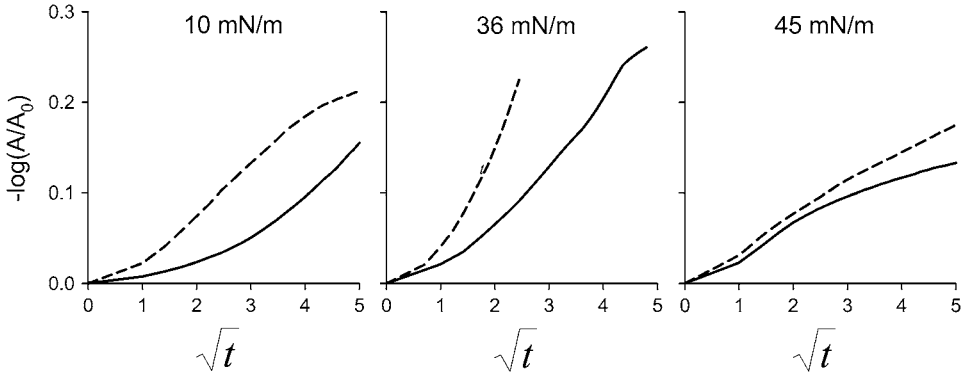

FIGURE 6 Constant pressure relaxation data of Re-LPS monolayers in the absence (*solid line*) and presence (*dashed line*) of 0.1 μg/mL SP-A, expressed as $-\log(A/A_0)$ vs. $\sqrt{t}$, to determine whether Re-LPS monolayer desorption is because of dissolution of Re-LPS molecules into the subphase or to monolayer transformation into 3D aggregates. A and A_0 are the trough surface areas at a given time, t, and at $t = 0$, respectively.

DISCUSSION

SP-A is known to cause bacterial aggregation and permeabilization (3–6). SP-A also permeabilizes model bacterial membranes composed of deep rough lipopolysaccharide (7). To our knowledge, the mechanism of SP-A-induced membrane permeabilization has not yet been reported. This study was undertaken to obtain further information on the mechanisms of SP-A-induced permeabilization of LPS membranes.

We found that SP-A favored the penetration of water molecules in Re-LPS membranes and caused a sharp decrease of the overall transition enthalpy of these membranes. Such SP-A effects might be due to either protein insertion into Re-LPS membranes or protein-induced perturbation of the lipid packing. Given that SP-A is a large oligomeric protein, it is unlikely that SP-A penetrates deeply into the Re-LPS membrane. Since SP-A strongly binds to Re-LPS (10,12), we hypothesize that SP-A perturbs Re-LPS acyl chain packing by taking up Re-LPS molecules from the membrane, reducing the number of Re-LPS molecules per unit of area. Using monolayer relaxation experiments at constant surface pressure, we demonstrated that SP-A induces Re-LPS molecular loss by promoting the formation of calcium-mediated protein aggregates that contain LPS (Figs. 3, 5, and 6). This would result in decreased van der Waals interactions between LPS hydrocarbon chains, consistent with SP-A-mediated decrease in the overall transition enthalpy of Re-LPS membranes observed by DSC (Fig. 1). These SP-A-induced packing defects would render the membrane leaky and allow the penetration of water molecules within the LPS membrane (Fig. 2).

Although the binding of SP-A to Re-LPS is independent of calcium (12,19), the presence of Ca^{2+} influences the interaction of SP-A with Re-LPS membranes in two ways: 1), Ca^{2+} binds tightly to the KDO moieties of Re-LPS (with an apparent dissociation constant of 14 μM) (27), neutralizing these negatively charged moieties, which minimizes electrostatic repulsions between SP-A and Re-LPS; and 2), Ca^{2+} induces self-aggregation of SP-A (13), and self-aggregated SP-A forms a network of interconnected filaments on Re-LPS monolayers (Fig. 3). Given that SP-A causes destabilization and area loss of Re-LPS monolayers in the presence of calcium (Figs. 4–6), it is reasonable to think that such large interconnected aggregates of fluorescently labeled TR-SP-A observed by epifluorescence microscopy represent supramolecular lipid-protein aggregates. The formation of such lattice-like structures on pure Re-LPS monolayers suggests that this might be the initial step in lesion formation in the outer membranes of Gram-negative bacteria induced by SP-A. Therefore, the formation of protein aggregates that contain LPS, rather than the formation of SP-A-induced discrete pores, might render the membrane leaky. This would be in agreement with the finding that the mechanism of SP-A-promoted bacterial membrane permeabilization is distinct from that of melittin (7), a well-known pore-forming peptide. On the other hand, in the presence of EDTA, SP-A neither formed aggregated structures nor affected Re-LPS relaxation kinetics, which indicates that SP-A's effects on Re-LPS membranes are strengthened by calcium.

In addition, we have shown that some SP-A-mediated processes, such as 1), Re-LPS molecular loss; 2), decrease of the overall transition enthalpy of Re-LPS membranes; and 3), increase of water penetration in Re-LPS membranes, were favored by the coexistence of gel and fluid lipid phases in these membranes. The presence of coexisting lipid domains within Re-LPS membranes would provide packing defects that facilitate the interaction of SP-A molecules with the lipid A moiety of Re-LPS, and the formation of extensive lattice-like structures at the interface depends on the specific interaction of SP-A with the lipid A part of bacterial lipopolysaccharide (19). In this study, lipid phase separation was induced by adding nonsaturating concentrations of calcium in the case of Re-LPS bilayers and by increasing surface pressure in the case of Re-LPS monolayers. On the other hand, it has been shown that incorporation of BPL in LPS membranes results in the formation of small BPL-enriched microdomains within the membrane (28). The presence of BPL in LPS bilayers confers susceptibility to antibiotic permeability because of structural modifications to the LPS membrane caused by BPL, leading to the formation of lipid phase separation (28,29). Moreover, the phospholipid/LPS ratio in the outer monolayer of the outer membrane of deep rough Gram-negative bacteria is larger than that of smooth

bacteria (30), making rough bacteria more sensitive to melittin (31) and to lung collectins (SP-A and SP-D) (3,4).

In summary, our results demonstrate that SP-A permeabilizes model bacterial membranes by forming calcium-dependent protein aggregates that may extract lipids from the membrane. In accordance with our findings, we propose a model in which SP-A binds onto the surface of Re-LPS membranes and covers it like a carpet. Calcium-induced self-aggregation of SP-A results in the accumulation of SP-A molecules on the surface of Re-LPS membranes. This high local protein concentration facilitates the formation of lipid-protein aggregates, which results in a loss of lipids from the membrane. As a consequence, transient defects are produced, rendering the membrane leaky.

This work was supported by the Ministerio de Educación y Ciencia (SAF2006-04434), Instituto de Salud Carlos III (CIBERES-CB06/06/0002), Comunidad Autónoma de Madrid (S-BIO-0260-2006), Fundación Médica MM, and Canadian Institutes of Health Research (CIHR MT-9361 to K.M.W.K.).

REFERENCES

1. Kuroki, Y., M. Takahashi, and C. Nishitani. 2007. Pulmonary collectins in innate immunity of the lung. *Cell. Microbiol.* 9:1871–1879.
2. Wright, J. R. 2005. Immunoregulatory functions of surfactant proteins. *Nat. Rev. Immunol.* 5:58–68.
3. Wu, H., A. Kuzmenko, S. Wan, L. Schaffer, A. Weiss, J. H. Fisher, K. S. Kim, and F. X. McCormack. 2003. Surfactant proteins A and D inhibit the growth of Gram-negative bacteria by increasing membrane permeability. *J. Clin. Invest.* 111:1589–1602.
4. Schaeffer, L. M., F. X. McCormack, H. Wu, and A. A. Weiss. 2004. Interactions of pulmonary collectins with *Bordetella bronchiseptica* and *Bordetella pertussis* lipopolysaccharide elucidate the structural basis of their antimicrobial activities. *Infect. Immun.* 72:7124–7130.
5. Zhang, S., Y. Chen, E. Potvin, F. Sanschagrin, R. C. Levesque, F. X. McCormack, and G. W. Lau. 2005. Comparative signature-tagged mutagenesis identifies *Pseudomonas* factors conferring resistance to the pulmonary collectin SP-A. *PLoS Pathog.* 1:259–268.
6. Zhang, S., F. X. McCormack, R. C. Levesque, G. A. O'Toole, and G. W. Lau. 2007. The flagellum of *Pseudomonas aeruginosa* is required for resistance to clearance by surfactant protein A. PLoS ONE 2:e564.
7. Kuzmenko, A., H. Wu, and F. X. McCormack. 2006. Pulmonary collectins selectively permeabilize model bacterial membranes containing rough lipopolysaccharide. *Biochemistry.* 45:2679–2685.
8. García-Verdugo, I., F. Sánchez-Barbero, F. U. Bosch, W. Steinhilber, and C. Casals. 2003. Effect of hydroxylation and N187-linked glycosylation on molecular and functional properties of recombinant human surfactant protein A. *Biochemistry.* 42:9532–9542.
9. Sanchez-Barbero, F. J. Strasser, R. Garcia-Canero, W. Steinhilber, and C. Casals. 2005. Role of the degree of oligomerization in the structure and function of human surfactant protein A. *J. Biol. Chem.* 280:7659–7670.
10. Sanchez-Barbero, F., G. Rivas, W. Steinhilber, and C. Casals. 2007. Structural and fuctional differences among human surfactant proteins SP-A1, SP-A2, and coexpressed SP-A1/SP-A2. Role of supratrimeric oligomerization. *Biochem. J.* 406:479–489.
11. Ruano, M. L., K. Nag, L. A. Worthman, C. Casals, J. Perez-Gil, and K. M. Keough. 1998. Differential partitioning of pulmonary surfactant protein SP-A into regions of monolayers of dipalmitoylphosphatidylcholine and dipalmitoylphosphatidylcholine/dipalmitoylphosphatidylglycerol. *Biophys. J.* 74:1101–1109.
12. Garcia-Verdugo, I., F. Sanchez-Barbero, K. Soldau, P. S. Tobias, and C. Casals. 2005. Interaction of SP-A (surfactant protein A) with bacterial rough lipopolysaccharide (Re-LPS), and effects of SP-A on the binding of Re-LPS to CD14 and LPS-binding protein. *Biochem. J.* 391:115–124.
13. Ruano, M. L., I. Garcia-Verdugo, E. Miguel, J. Perez-Gil, and C. Casals. 2000. Self-aggregation of surfactant protein A. *Biochemistry.* 39:6529–6537.
14. Canadas O., R. Guerrero, R. Garcia-Canero, G. Orellana, M. Menendez, and C. Casals. 2004. Characterization of liposomal tacrolimus in lung surfactant-like phospholipids and evaluation of its immunosuppressive activity. *Biochemistry.* 43:9926–9938.
15. Saenz, A., O. Canadas, L. A. Bagatolli, M. E. Johnson, and C. Casals. 2006. Physical properties and surface activity of surfactant-like membranes containing the cationic and hydrophobic peptide KL4. *FEBS J.* 273:2515–2527.
16. Saenz, A., O. Canadas, L. A. Bagatolli, F. Sanchez-Barbero, M. E. Johnson, and C. Casals. 2007. Effect of surfactant protein a (SP-A) on the physical properties and surface activity of KL_4-surfactant. *Biophys. J.* 92:482–492.
17. Azumi, T., and S. P. McGlynn. 1962. Polarization of the luminescence of phenantrene. *J. Chem. Phys.* 37:2413–2420.
18. Nag, K., C. Boland, N. Rich, and K. M. Keough. 1991. Epifluorescence microscopic observation of monolayers of dipalmitoylphosphatidylcholine: dependence of domain size on compression rates. *Biochim. Biophys. Acta.* 1068:157–160.
19. Garcia-Verdugo, I., O. Canadas, S. G. Taneva, K. M. W. Keough, and C. Casals. 2007. SP-A forms extensive lattice-like structures on DPPC/rough-lipopolysaccharide mixed monolayers. *Biophys. J.* 93:3529–3540.
20. Worthman, L. A., K. Nag, N. Rich, M. L. Ruano, C. Casals, J. Pérez-Gil, and K. M. Keough. 2000. Pulmonary surfactant protein A interacts with gel-like regions in monolayers of pulmonary surfactant lipid extract. *Biophys. J.* 79:2657–2666.
21. Roes, S., U. Seydel, and T. Gutsmann. 2005. Probing the properties of lipopolysaccharide monolayers and their interaction with the antimicrobial peptide polymyxin B by atomic force microscopy. *Langmuir.* 21:6970–6978.
22. Nikaido, H., and M. Vaara. 1985. Molecular basis of bacterial outer membrane permeability. *Microbiol. Rev.* 49:1–32.
23. Vollhardt, D. 1993. Nucleation and growth in supersaturated monolayers. *Adv. Colloid Interface Sci.* 47:1–23.
24. Vollhardt, D. 2006. Nucleation in monolayers. *Adv. Colloid Interface Sci.* 123–126:173–188.
25. Smith, R. D., and J. C. Berg. 1980. The collapse of surfactant monolayers at the air—water interface. *J. Colloid Interface Sci.* 74:273–286.
26. Garidel, P., M. Rappolt, A. B. Schromm, J. Howe, K. Lohner, J. Andra, M. H. J. Koch, and K. Brandenburg. 2005. Divalent cations affect chain mobility and aggregate structure of lipopolysaccharide from *Salmonella minnesota* reflected in a decrease of its biological activity. *Biochim. Biophys. Acta.* 1715:122–131.
27. Schindler, M., and M. J. Osborn. 1979. Interaction of divalent cations and polymyxin B with lipopolysaccharide. *Biochemistry.* 18:4425–4430.
28. Tong, J., and T. J. McIntosh. 2004. Structure of supported bilayers composed of lipopolysaccharides and bacterial phospholipids: raft formation and implications for bacterial resistance. *Biophys. J.* 86: 3759–3771.
29. Snyder, D. S., and T. J. McIntosh. 2000. The lipopolysaccharide barrier: correlation of antibiotic susceptibility with antibiotic permeability and fluorescent probe binding kinetics. *Biochemistry.* 39:11777–11787.
30. Vaara, M., W. Z. Plachy, and H. Nikaido. 1990. Partitioning of hydrophobic probes into lipopolysaccharide bilayers. *Biochim. Biophys. Acta.* 1024:152–158.
31. Allende, D., and T. J. McIntosh. 2003. Lipopolysaccharides in bacterial membranes act like cholesterol in eukaryotic plasma membranes in providing protection against melittin-induced bilayer lysis. *Biochemistry.* 42:1101–1108.